Polymer 79 (2015) 29–36

Contents lists available at ScienceDirect

Polymer

journal homepage: www.elsevier.com/locate/polymer

Synthesis and structure formation in dilute aqueous solution of a chitosan-DNA hybrid

Ilyès Safir [a], Kien Xuan Ngo [a], Jancy Nixon Abraham [a], Majid Ghahraman Afshar [a], Ewa Pavlova [b], Corinne Nardin [a, *]

[a] University of Geneva, Faculty of Sciences, Department of Inorganic and Analytical Chemistry, Quai Ernest Ansermet 30, 1211, Geneva 4, Switzerland
[b] Institute of Macromolecular Chemistry, Academy of Sciences of the Czech Republic, Heyrovsky Sq. 2, 162 06, Prague 6, Czech Republic

ARTICLE INFO

Article history:
Received 16 April 2015
Received in revised form
24 September 2015
Accepted 27 September 2015
Available online 30 September 2015

Keywords:
Chitosan
DNA
Self-assembly

ABSTRACT

In the following is described the combination of straight biochemical and organic routes to graft nucleotide sequences to a chitosan backbone. The resulting chitosan-g-ssDNA hybrid self-assembles into submicrometer size structures in dilute aqueous solution as assessed by atomic force and electron microscopy imaging. The hypothesis of self-assembly driven by chemical incompatibility between the amphiphilic chitosan and nucleic acid grafts is supported further by stability of the self-assembly against ionic strength and pH variations.

1. Introduction

Chitosan is a polymer that mainly results from the deacetylation of natural chitin, which is extracted for instance from shrimp shells or squid pens. Chitosan is a complex linear amphiphilic copolymer composed of glucosamine and N-acetyl glucosamine residues, which are statistically distributed along the chain [1]. Its glass transition temperature is not accessible before thermal decomposition. The case of oligomers remains complex as well. Chitosan in aqueous solution is an amphiphilic polyelectrolyte [2]. The degree of acetylation (DA) along with the distribution of the two residues, the degree of polymerization as well as the index of polydispersity (Ip) and the contour length affect the electrostatic potential of the polymer chain. Below a DA of 60%, chitosan is soluble in dilute acidic media. Below a DA of 28%, the polymer is a strong polyelectrolyte, which is fully charged at pH around 4.5 [1–3].

Although complex, chitosan is an interesting substitute for synthetic polymers owing to both its biological and mechanical properties [2]. Chitosan is a unique natural cationic polymer that undergoes interpolyelectrolyte complex formation with anionic polyelectrolytes [1,4]. Upon copolymerization, it might self-assemble into core–shell structures in the sub-micrometer size range. Towards this end, synthesis routes are being devised to graft polymer segments to chitosan. Most investigations are carried out for potential medical applications in either drug [5–9] or gene delivery [10,11]. For instance, owing to the degradability and biocompatibility of poly(ethylene oxide)-b-poly(lactic acid)-b-poly(ethylene oxide) (PEO-PLLA-PEO), this copolymer has been grafted to chitosan through a combination of click chemistry and single electron transfer-nitroxide radical coupling (SET-NRC) [12]. Emulsion was used as well to synthesize a poly(lactic-co-glycolic acid) amphiphilic macromolecule that self-assembles into micelles [13]. Since these polymers can self-assemble into micelles, reduction sensitive graft copolymers composed of chitosan and

Abbreviations: Chitosan-*grafted*-single stranded DNA, Chitosan-g-ssDNA; degree of acetylation, DA; controlled pore glass, CpG; gel permeation chromatography, GPC; 2-(N-morpholino)ethanesulfonic acid buffer, MES; N-hydroxysuccinimide, NHS; 1-ethyl-3-(3-dimethylaminopropyl) carbodiimide hydrochloride, EDC; matrix-assisted laser desorption/ionization time of flight, MALDI-TOF; 2,5-dihydroxybenzoic acid matrix, DHB; analytical ultra-centrifugation, AUC; transmission electron microscopy, TEM; atomic force microscopy, AFM; poly(ethylene imine), PEI; deacetylation degree, DD; ultraviolet, UV; right angle laser light scattering, RALS; low angle laser light scattering, LALS; refractive index, RI; tetrahydrofuran, THF; retention volume, V_R.

* Corresponding author. Current address: Université de Pau et des Pays de l'Adour, IPREM/EPCP, Technopole Helioparc, 2, av. Pdt Angot, 64 053 PAU cedex 09, France.
E-mail addresses: corinne.nardin@unige.ch, Corinne.nardin@univ-pau.fr (C. Nardin).

http://dx.doi.org/10.1016/j.polymer.2015.09.072
0032-3861/

poly (ε-caprolactone) are of interest for drug delivery as well [14].

We previously reported the coupling of synthetic nucleotide sequences to soft, hydrophobic synthetic polymers [15–17] and to short peptide sequences [18]. Owing to the incompatibility between the water soluble flexible nucleotide sequence and the hydrophobic polymer or peptide segment, the resulting diblock copolymers undergo either self-assembly [14,15,17a] or nucleation polymerization into amyloid-like fibres [16,17b,17c]. A nucleic acid strand might however undergo several modes of interaction, in particular electrostatic interaction. Keeping in mind their potential for application in biology or medicine and for the comprehension of the role of inter- and intramolecular interactions on the mechanism of structure formation of DNA-copolymers, we report herein on the coupling of nucleic acid grafts along a chitosan backbone. The presence of the chargeable amine groups along the polymer segment would enable the investigation of the role of inter- and intramolecular electrostatic interaction on the structure formation of the resulting chitosan-g-ssDNA hybrid. Moreover, structure formation is expected to be sensitive to pH and ionic strength owing to the dependence on pH of the solubility of chitosan. As described in the following, the combination of biochemical and organic routes evidence the grafting of one nucleic acid strand to a chitosan backbone as assessed by conventional chemical characterization techniques. The resulting chitosan-g-ssDNA hybrid self-assembles into submicrometer size spherical structures as evidenced by atomic force and electron microscopy imaging, the size of which is not sensitive to ionic strength or pH variations. The submicrometer size spherical structures self-assemble owing to incompatibility between the water soluble, flexible single stranded nucleotide sequence and the non water soluble chitosan segment.

2. Material and methods

2.1. Materials

Chitosan was purchased from Sigma Aldrich (Buchs, Switzerland) with a deacetylation degree (DD) above 75% (D. A. below 25%) and a molecular weight (M_w) between 50,000 and 160,000 Da. Papain (1.3 U mg^{-1} at pH 6.2 and 25 °C) was purchased from Sigma Aldrich (Buchs, Switzerland). The single stranded nucleotide sequence (ssDNA) modified at the 5′-end through a decyl spacer with a carboxylic acid group (5′-CTCTCTCTCTTT-3′, 5′-$(CT)_5T_2$-3′, C stands for cytosine and T for thymine) was purchased on controlled pore glass (CpG) (desalted, M_w 3763.9) from Microsynth (Balgach, Switzerland). The complementary sequence without any modification (5′-AAAGAGAGAGAG′-3, 3'-$(GA)_5A_2$-5′, G stands for Guanine and A for Adenine, desalted, Mw 3776.2) was also purchased from Microsynth. N-hydroxysuccinimide (NHS), 1-ethyl-3-(3-dimethylaminopropyl) carbodiimide hydrochloride (EDC), 2-(N-morpholino)ethanesulfonic acid (MES) buffer and dialysis tubes (MWCO 2000), were purchased from Sigma Aldrich (Buchs, Switzerland). The ammonia solution 35% was purchased from Fisher Scientific SA (Wohlen, Switzerland). Polyacrylamide beads (Bio-Gel medium), fractionating range varying from 1500 to 20,000 Mw were purchased from BioRad AG (Cressier, Switzerland). Other chemicals such as salts and organic solvents were purchased from Sigma Aldrich, Fluka (Cressier, Switzerland), GE Healthcare (Glattbrugg, Switzerland), Acros Organics (Geel, Belgium), BioRad (Hercules, USA), and used without further purification. Mica was purchased as high-grade quality V1, from Plano GmbH, (Wetzlar, Germany). Polystyrene analytical standard in a broad range of molecular weight used to calibrate the GPC system were purchased from PolyCAl™ PS Std from Malvern Instruments Ltd (Malvern, UK). Ultrapure THF used as the mobile phase for GPC was purchased from HiperSolv CHROMANORM via Sigma Aldrich (Buchs, Switzerland).

2.2. Methods

2.2.1. Enzymatic digestion of chitosan

Chitosan was digested by papain in order to get low M_w polymer prior to grafting to ssDNA according to previously published reports [19]. Chitosan (10 mg mL^{-1}) was dissolved in 100 mL of acetate buffer (10 mM, pH 4.5). Papain (1.3 U mg^{-1}) was then added to the chitosan solution (10 mL) to a final concentration of 0.1 mg mL^{-1} and the enzymatic reaction was initiated at 45 °C and continued for 24 h. The reaction was stopped by increasing the temperature to 100 °C for 10 min, in order to deactivate the enzyme. The fractions of chitosan digested by papain were separated and collected by size exclusion chromatography (SEC) on a Sephadex G-50 gel medium on an Econo-column (Bio-Rad, 1 × 50 cm). The 1% acetic acid, pH = 3 elution solvent was degassed prior to use.

2.2.2. Synthesis of chitosan-grafted-ssDNA

The chitosan-grafted-ssDNA copolymer was synthesized in two steps. At first, 100 mg of resin (3.7 μmol, M_w 3763.9) was dissolved in 700 μL of 2-(N-morpholino)ethanesulfonic acid buffer (MES) (0.1 M, pH = 4.9) with N-hydroxysuccinimide (NHS), (Mw 115.09, 8.6 μmol) and 1-ethyl-3-(3-dimethylaminopropyl) carbodiimide hydrochloride (EDC) (Mw 155.24, 6.4 μmol). The reaction was carried out in a thermal shaker (Thermo-shaker, Grant-bio, VDC Faust, Geneva, Switzerland) for 2 h at room temperature to enable the activation of the ssDNA carboxylic acid groups. In a second step the chitosan (Mw ≈ 4500, 6.6 μmol) was added to the reactor and the reaction carried out for 24 h at room temperature under 1200 rpm shaking overnight in a thermal shaker. The excess reagents were removed by rinsing with MES buffer (30 mL). The chitosan-grafted-ssDNA on solid support was cleaved from the resin by addition of 1.0 mL of a 35% ammonia solution. This reaction was performed in a thermal shaker and maintained at 40 °C for 24 h. The copolymer was then filtered to remove the resin, and the resin was further washed with water.

Chitosan-grafted-ssDNA was purified by SEC to remove any unreacted DNA subsequent to synthesis on an Econo-column (1 × 50 cm) loaded with the Bio-Gel P-10 gel medium. The 2-(N-morpholino)ethane sulfonic acid buffer (MES) (0.1 M, pH = 4.9) elution buffer was used as eluent.

The chitosan-grafted-ssDNA copolymer was subsequently dialysed against milliQ water at room temperature (2000 MWCO dialysis membrane) to remove remaining salts and protecting groups and finally, the copolymer was lyophilized using a speed vac SC110 device (Ramsey, USA).

2.2.3. Gel permeation chromatography

GPC was carried out with the Viscotek instrument (Malvern Instruments Ltd, UK) controlled by the OmniSec 4.7 software supplied by Viscotec. The instrument is equipped with a VE 122 solvent delivery system, a manual injector equipped with a 100 μL loop, a VE 7510 GPC degasser and a multi detector system including UV (270 dual detector), RI, RALS and LALS detectors. Separations were performed on a Viscotec TGuard Org Guard Co I 10 × 4.6 mm (No. A208034) pre-column and a Viscotek T6000M General Mixed Org 300 × 8.0 mm (No. C111525) column.

Isocratic analysis was performed at 1.0 mL min^{-1} flow rate with ultrapure THF. The mobile phase was filtered through 0.45 μm membrane filters. Prior to injections, the column was equilibrated for at least 30 min by THF flowing through the system to obtain a stable baseline. The polystyrene standards, chitosan and chitosan-g-ssDNA were dissolved in THF and the solution of chitosan and chitosan-g-ssDNA were acidified in order to overcome the

solubility issue prior to the injection. The calibration curve was performed using thirteen various molecular weights of polystyrene analytical standards. The calibration plot (logarithm molecular weight M_w versus retention volume V_R) was achieved by replicate analysis (n = 3) with all molecular weights and the linear relationship was evaluated using the least square method (log Mw = −0.47 V_R + 9.27, r^2 = 0.99).

2.2.4. Proton nuclear magnetic resonance (^{1}H NMR)

^{1}H NMR measurements were carried out at room temperature using the AMX-500 Bruker NMR spectrometer operating at 500 MHz (Rheinstetten, Germany). Chitosan was dissolved in deuterium oxide (D_2O) and 2% of deuterium chloride (DCl) at a concentration of 3 mg mL^{-1}. The DA of chitosan was determined using the following equation [20]:

$$\boldsymbol{DA} = \left[\left(1/3 \times \boldsymbol{I}_{\boldsymbol{CH}_3}\right)/\left(1/6 \times \boldsymbol{I}_{(\boldsymbol{H}_2-\boldsymbol{H}_6)}\right)\right] \times 100 \quad (1)$$

I_{CH_3} corresponds to the integration of the signal of *N*-acetyl glucosamine (GlcNAc) and $I_{(H2-H6)}$ to the summation of the integrals of the signals of H_2, H_3, H_4, H_5, and H_6.

2.2.5. Matrix-assisted laser desorption/ionization time of flight (MALDI-TOF)

MALDI-TOF was used to characterize the chitosan after enzymatic digestion and the chitosan-g-ssDNA copolymer. Chitosan was dissolved in MES buffer and the copolymer in an aqueous solution of acetonitrile (70/30 acetonitrile/H_2O v/v ratio) using 2,5-dihydroxybenzoic acid (DHB) as matrix (Sigma Aldrich, Buchs, Switzerland).

2.2.6. Analytical ultra centrifugation (AUC)

Analytical ultracentrifugation (AUC) was performed on an Optima XL-I ultracentrifuge (Beckmann-Coulter, Palo Alto, CA) equipped with Rayleigh interference optics. Sedimentation–velocity experiments were performed with 1 mg mL^{-1} solutions of chitosan, DNA and Chitosan-g-ssDNA copolymer in water/ethanol 1:1 (v/v) at a rotational speed of 50 krpm at 25 °C.

2.2.7. Self-assembly of chitosan-g-ssDNA copolymer in water

The lyophilized powder of the chitosan-g-ssDNA copolymer was dissolved in a solvent mixture of acetonitrile/water (70/30 v/v), at a concentration of 1 mg mL^{-1}. A volume of 200 μL of solution was dialysed (2000 MWCO) over night against milliQ water to fully exchange the amount of acetonitrile with water.

2.2.8. Microscopy imaging

Imaging in the dry state by atomic force microscopy (AFM) was performed with an MFP-3D microscope (Asylum Research, Santa Barbara, CA, USA) equipped with two optical microscopes (Zeiss, Göttingen, Germany). The measurements carried out in the liquid state were performed on a Cypher™ atomic force microscope (Asylum Research, Santa Barbara, CA, USA). Mica surfaces (dimension of 0.5 × 0.5 cm) were cleaned by removing one sheet with an adhesive tape. A sample volume of 20 μL of self-assembled chitosan-g-ssDNA (1 mg mL^{-1}) in aqueous solution was dropped over the surface and left for drying overnight at room temperature before imaging. To immobilize the structures on the mica substrate, 30 μL of a PEI solution prepared at a concentration of 5 ppm was drop casted on a mica surface for 20 min. Subsequent washing with milliQ water was performed to remove unbound PEI. Self-assembled chitosan-g-ssDNA was then drop casted on functionalized mica and kept over 20 min prior to washing with milliQ water to remove unbound chitosan-g-ssDNA. All images were acquired in the AC mode in air at room temperature, with silicon nitride tips on soft cantilevers (model Olympus, Tokyo, Japan) purchased from Asylum Research, having a resonance frequency of 69 kHz and spring constant of 2 N m^{-1} at a scan rate of 0.9 Hz. The data analysis was done using the Igor software provided with the equipment.

Transmission electron microscopy (TEM) and cryogenic transmission electron microscopy (Cryo-TEM) were performed with a Tecnai Spirit Twin 12 microscope (FEI, Czech Republic), equipped with a Gatan cryo-specimen holder in the bright field-imaging mode at 120 kV accelerating voltage.

For transmission electron microscopy (TEM), samples were prepared by dropping a small amount of sample (volume: 2 μL; concentration: 1 mg mL^{-1}) on a TEM copper grid (300 mesh), which was coated with a thin, electron-transparent carbon film. The excess of solution was removed out by touching the bottom of the grid with filter paper. This fast removal of the solution was performed after 1 min in order to minimize oversaturation during the drying process. Both samples were left to dry completely at room temperature, transferred to the TEM microscope and observed at 120 kV.

For Cryo-TEM imaging, sample preparation consisted in dropping 3 μL of the sample solution on a TEM grid covered with a holey carbon supporting film (C-flat 2/1-4C, Electron Microscopy science; Hatfield, England); just before the experiment, the film was rendered hydrophilic by glow discharge (Expanded Plasma Cleaner; Harrick Plasma, USA). The excess of the solution was removed by blotting (blotting time 1 s; Whatman no. 1 filter paper) and the grid was immediately plunged into liquid ethane held at −181 °C. The frozen sample was transferred into the microscope and observed at −173 °C at 120 kV.

2.2.9. Dynamic light scattering (DLS)

Mutual hydrodynamic diameters (D_m) were measured by dynamic light scattering (DLS) at 25 °C using the Zetasizer Nano Series from Malvern Instruments (Malvern, United Kingdom) at a backscattered angle of 173 °C in optically homogeneous square polystyrene cells.

The zeta potential of low M_w chitosan was measured by the micro electrophoretic method using a Malvern Zetasizer Nano ZS apparatus (Malvern, United Kingdom).

Sizes of the chitosan-g-ssDNA self-assembled structures were measured at pH 7 at a concentration of 1 mg mL^{-1} whereas sizes of the structures resulting from the non-covalent, electrostatic interaction between ssDNA and chitosan could only be monitored in acidic aqueous solutions at pH 5, at a concentration of 1 mg mL^{-1}. At higher pH, the chitosan precipitates. The size of the single stranded DNA modified with the decyl spacer was measured in aqueous solution at pH 7 at a concentration of 1 mg mL^{-1}.

3. Results and discussion

Chitosan is a polymer mainly derived from the natural chitin, which is by now widely used in applications such as dental, buccal, gastrointestinal drug delivery and gene delivery due to its favourable biological properties [15–17]. The attractive characteristics of this amino-polysaccharide (biodegradable, biocompatible, antioxidant, antimicrobial, antitumour and positively charged nontoxic mucoadhesive biopolymer [14]) are however weakened by its solubility in aqueous solution of pH below 4.5 solely, which limits its use although it is the second most abundant natural polysaccharide. Grafting to a nucleic acid strand would therefore enable the synthesis of an amphiphilic copolymer that would undergo structure formation at neutral pH. Moreover, newly synthesized compounds based on synthetic nucleic acids have shown promising results as potential drugs [21]. Conjugation indeed enhances the

limited intracellular delivery of nucleotide sequences whereas DNA-copolymer structure formation into spherical core–shell micelles or vesicles is of high potential for drug delivery. DNA indeed enables the convenient and fast generation of multifunctional particles whereas a hydrophobic core could be loaded with hydrophobic anticancer drugs for instance. The additional advantage of chitosan over other polysaccharides is that its chemical structure allows specific modifications at the C-2 position of the amine group to enable the formation of an amide bond between these amino groups and activated carboxylic groups [14]. Hence specific groups can be introduced to design copolymers for selected applications.

Commercially available high Mw Chitosan is therefore at first digested by enzymatic degradation to achieve a low molecular weight polymer according to previously published routes [14] so that the resulting copolymer might be of sufficient solubility to undergo structure formation in aqueous solution. The resulting low molecular weight chitosan has been characterized by SEC and ^{1}HNMR (Figs. S1a and S2) respectively. The peak at 2.2–2.4 ppm in the ^{1}HNMR spectrum is assigned to the three protons of *N*-acetyl glucosamine (GlcNAc), and the peak at 3.4–3.6 ppm to the H_2 proton of glucosamine (GlcN) residues. The peaks at 3.9–4.3 ppm correspond to the cumulative signals of the H_2, H_3, H_4, H_5, and H_6 protons of glucosamine (GlcN) and the peak at 5.0–5.2 ppm is assigned to the proton H_1 of glucosamine (GlcN). The degree of acetylation (DA) could thus be evaluated to 3.8%. Hence, the constants (Scheme 1) are y=3.8, x= 5.3 and z=90.9.

The nucleotide sequence is a linear 12-mer of Cytosine and Thymine chosen in order to assemble a thermodynamically stable double helix by hybridization with its complementary strand at room temperature. To avoid tedious chemistry and purification steps, coupling of chitosan and nucleic acid strands is performed on solid support. Grafting of the nucleotide strand to the chitosan was performed by solid phase supported synthesis with nucleic acid sequences functionalized with a carboxylic acid group at the 5′-end. An amide bond is thus formed with the dangling amino groups available along the chitosan backbone (Scheme 1).

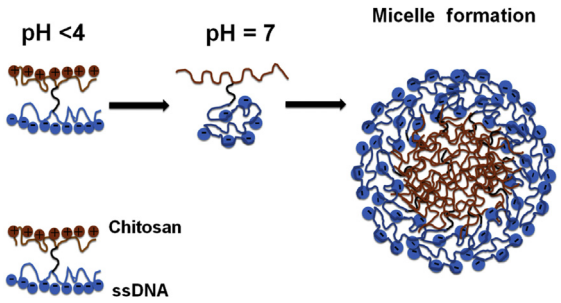

Scheme 2. Schematic representation of chitosan-grafted-ssDNA structure formation.

SEC of the resulting chitosan-g-ssDNA evidences separation of the copolymer from the unreacted nucleotide sequences (Fig. S1b). Successful synthesis and purification of the chitosan-grafted-ssDNA copolymer is further evidenced by analytical ultracentrifugation

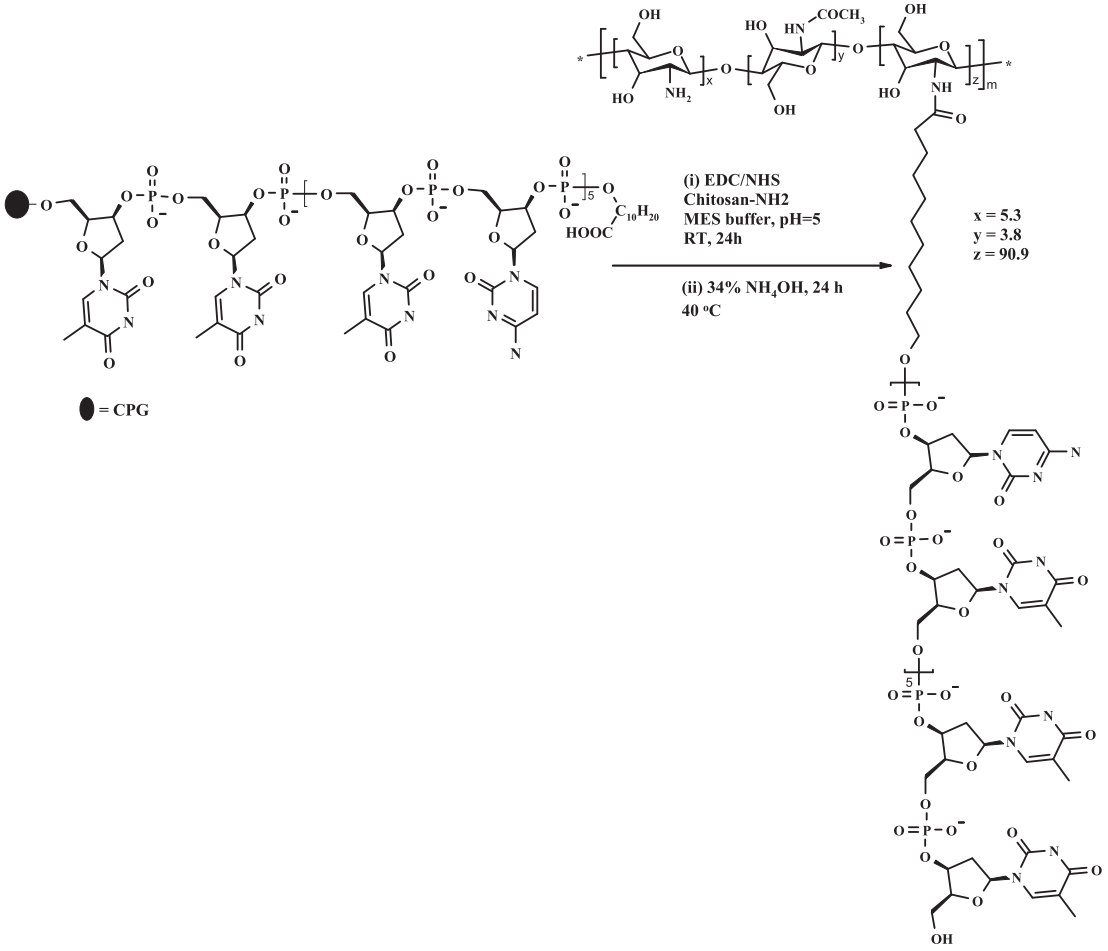

Scheme 1. Synthesis scheme of chitosan-grafted-ssDNA.

(AUC), (Fig. S3); which reveals single traces for chitosan, single stranded DNA (ssDNA) and the chitosan-grafted-ssDNA. Sequential enzymatic digestion of chitosan and coupling to the nucleic acid strand enables achieving a copolymer with a reaction yield of about 40%.

Molecular mass determination was achieved at first by MALDI-TOF spectrometry. As can be observed in Figs. S4a and S4b, average molecular masses of 4425 Da and 3771 Da were monitored for chitosan (1.3 PDI) and ssDNA (in agreement with the expected value, i.e. 3763.9 Da provided by the supplier). Subsequent to coupling, the chitosan-grafted-ssDNA copolymer mass is of 7908 Da (Fig. S4c). This value is in close agreement with a copolymer mass of 8243 Da at a 1:1 M grafting ratio. GPC was further used to determine the apparent molecular weight of both chitosan and chitosan-g-ssDNA. As seen in Fig. 1a, linearity between the molecular weight (M_w) and the retention volume (V_R) in the molecular mass range of interest enables the accurate determination of the apparent molecular weight of the polymers of interest [22]. Retention volumes of 11.96 and 11.42 mL for chitosan [23] and chitosan-g-ssDNA (See Fig. 1b and Fig. S5) yield molecular weights of 4511 and 8092 Da for chitosan and chitosan-g-ssDNA respectively, in good agreement with masses determined by MALDI-TOF. The minor distribution characterized by a broad shoulder between 11.55 and 11.95 indicates the presence of little amount of unmodified chitosan.

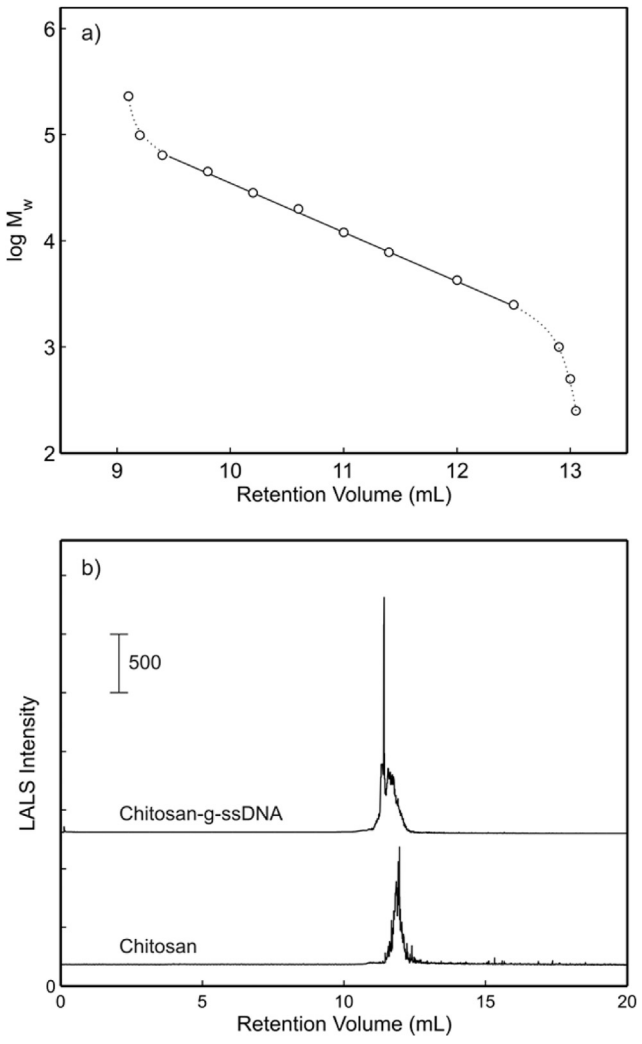

Fig. 1. a) GPC calibration curve. b) GPC chromatograms of chitosan and chitosan-g-ssDNA (LALS response).

Due to both chemical and physical incompatibility between the rigid amphiphilic chitosan polymer and the flexible hydrophilic ssDNA, structure formation of the chitosan-g-ssDNA hybrid was induced in water by solvent displacement through dialysis [24]. Towards this end, the chitosan-g-ssDNA was dissolved in an aqueous solution of acetonitrile, which was further dialysed against water. Imaging by AFM in the dried state reveals that the chitosan-g-ssDNA copolymer is molecularly dissolved in acetonitrile/water.

To resolve the morphology of the resulting self-assembled chitosan-g-ssDNA structures in aqueous solution, AFM measurements were performed in the dry and liquid states. Representative results are displayed in Fig. 2. AFM imaging among twenty structures in the dried state evidences that the chitosan-g-ssDNA self-assembles into spherical structures of (57 ± 12) nm average size and (11 ± 2) nm average height. To rule out any drying artefacts, morphological analysis was further performed by AFM in the liquid state. As observed in Fig. 2c, the spherical morphology is retained and structures of about (61 ± 25) nm size and (22 ± 15) nm in height (Fig. 2d) are observed. The difference in height in both environments (dry and liquid) arises from the fact that in the dry state, structures certainly have undergone drying that induces their flattening, which is indicative of their softness.

These were further characterized by transmission electron microscopy (TEM). The structures exhibited sufficient contrast without staining. As displayed in Fig. 3, TEM and Cryo-TEM imaging revealed the presence of spherical structures with sizes of (44 ± 10) nm and (52 ± 18) nm respectively. Cryo-TEM and AFM performed in the liquid state thus reveal structures of about 50 nm size. Unfortunately, the low refractive index increment (8.31×10^{-6} cm^3 mg^{-1}) of the system prevents characterization by static light scattering. We could however resort to centrifugation to sort out the few larger structures that could prevent accurate sizing by dynamic light scattering. Chitosan-g-ssDNA self-assembles into structures of (103 ± 10) nm apparent diameter (see Fig. S6a). Noteworthy is the monomodal distribution subsequent to centrifugation. The chitosan-g-ssDNA micelles are of smaller size than the complexes formed by non-covalent electrostatic interaction between the oppositely charged chitosan and nucleic acid sequences assembled at pH 5, i.e. 255 nm (Fig. S6b) and than the decyl modified ssDNA, i.e. 190 nm (Fig. S6 C).

To establish the mechanism of structure formation, the effect of hydrogen bonding on self-assembly was assessed at first. Either the complementary sequence was added to the solution of molecularly dissolved chitosan-g-ssDNA in acetonitrile/water prior to induce self-assembly or the complementary sequence was added subsequent to the self-assembly of the chitosan-g-ssDNA. In both cases, the complementary nucleic acid strands were added at 1:1 M ratio. In Fig. 4 are displayed representative AFM images obtained in the dry state of the resulting self-assembled structures in presence of the complementary sequence. If the complementary sequence is added to the aqueous solution of acetonitrile prior to dialysis, the structures in comparison to those assembled in the absence of the complementary sequence appear similar in shape and size (40 ± 2 nm). Interestingly, polydispersity decreased. However, although the hydrophilic weight fraction is increased by hybridization, no morphological transition could be observed, probably balanced by the increased rigidity and charge of the hybridized hydrophilic sequences in comparison to that of the pristine single stranded nucleic acid sequence.

Upon hybridization subsequent to structure formation, the specific hydrogen bonds between the complementary sequences did not affect the intermolecular interactions, which drive structure formation. As can be observed in Fig. 4, although the size is affected,

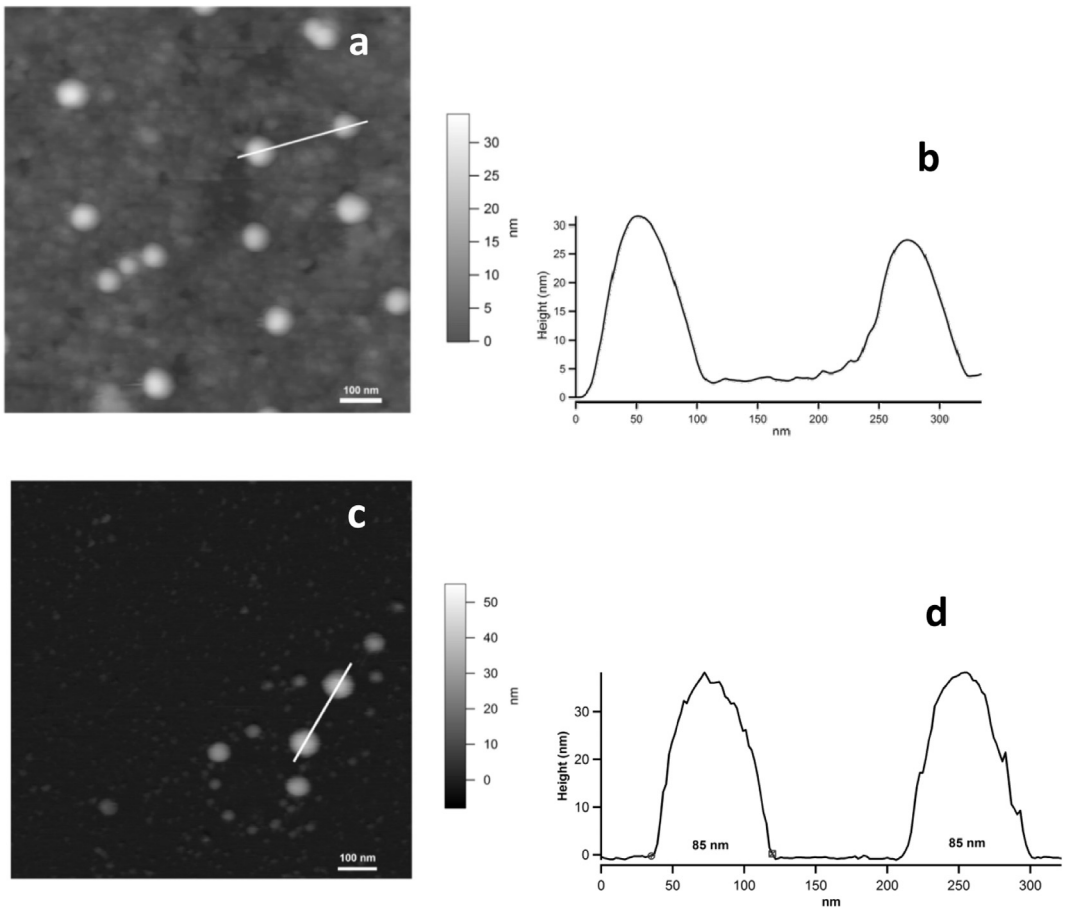

Fig. 2. AFM imaging of chitosan-g-ssDNA self-assembled structures immobilized on mica a) in the dry state, b) Corresponding height profile, c) in liquid in 1 mM NaCl ionic strength; d) corresponding height profile.

the morphology is retained which indicates that hydrogen bonding between the chitosan-g-ssDNA hybrids participate in the self-assembly but is not driving structure formation. The average size assessed among twenty self-assembled chitosan-g-ssDNA structures is of about (251 ± 57) nm. Although swelling (by a factor of three) is induced, self-assembly is not hindered and no morphological transition is observed. The hydrophobic interaction obviously remains the driving force to stable self-assembly.

Of high interest is that the self-assembly is not sensitive to either pH as assessed by characterization in a medium of pH 1.5 (Fig. S7) or to the ionic strength (Fig. 5), which further proves that hydrophobic interaction is the main driving force to structure formation. AFM liquid imaging was performed at first in a 1 mM NaCl aqueous solution. In a second step solution exchange was performed in situ to increase the ionic strength to 150 mM NaCl for 15 min prior to imaging. Only the largest chitosan-g-ssDNA structures opened and a homogenous layer of 6 nm thickness formed. Assuming the length of the ssDNA fragment to be of about 4 nm and that of chitosan of about 2 nm [25], the thickness of the layer is matching that of a polymer monomolecular film (see Fig. 5).

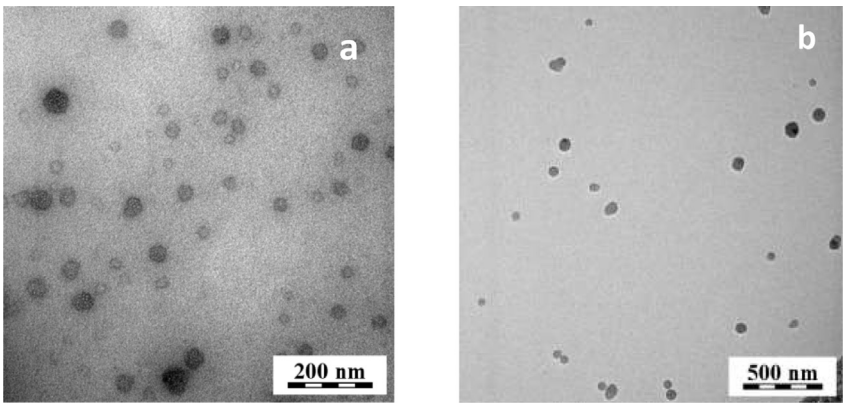

Fig. 3. a) TEM and b) Cryo-TEM imaging of chitosan-g-ssDNA self-assembled structures.

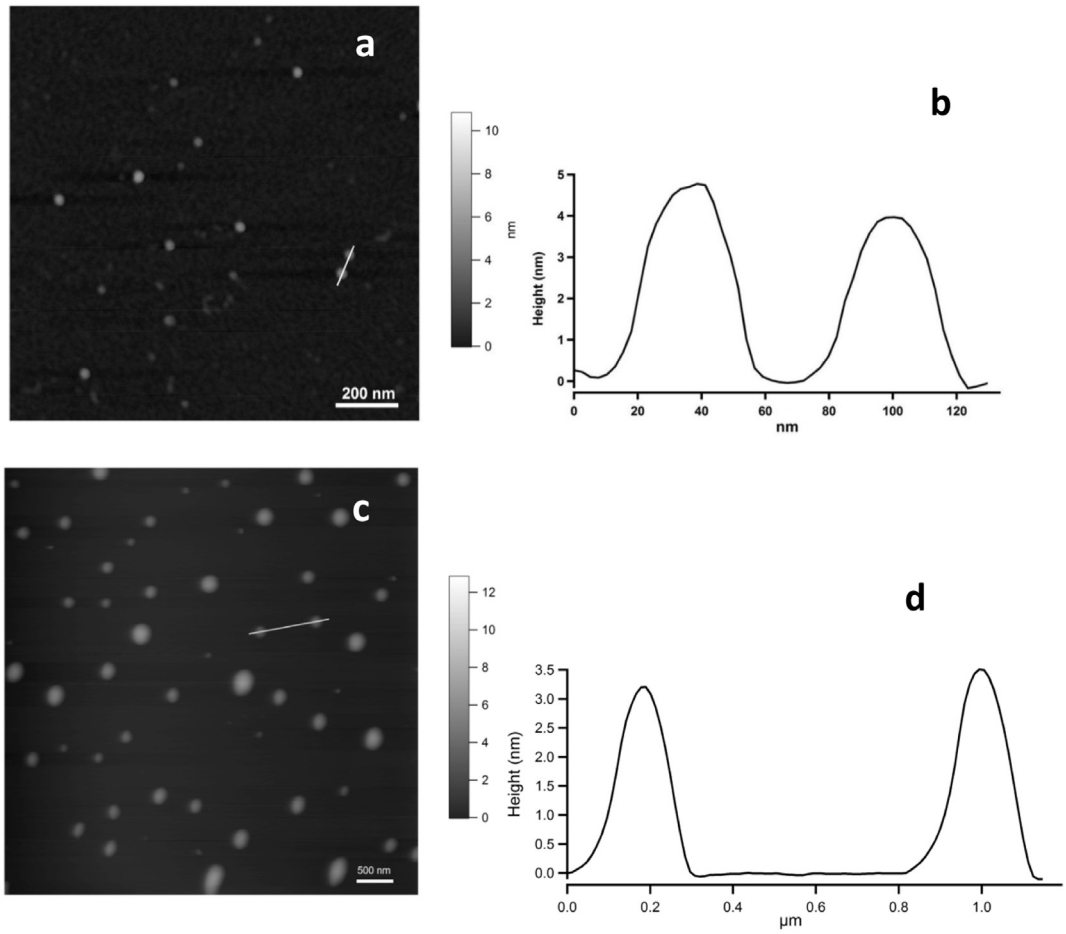

Fig. 4. a) Structure formation upon hybridization with the complementary sequence added before solvent displacement, b) subsequent to self-assembly as observed by AFM.

Formation of a thin film upon increasing the ionic strength could however only be observed with the largest structures.

This result is indicating that chitosan-grafted-ssDNA undergoes structure formation driven by the chemical and physical incompatibility between the rigid, amphiphilic chitosan and the flexible, water soluble nucleic acid sequences. This assumption is further supported by zeta-potential values. In an aqueous neutral medium, the value was of about −1.8 mV. The surface charge of the structures can be considered as slightly negative because of the negative phosphate groups along the nucleic acid sequence which composes the micellar corona. The chitosan precipitates at pH 7.4. It is hydrophobic and composes the core of the micelles. Chitosan is

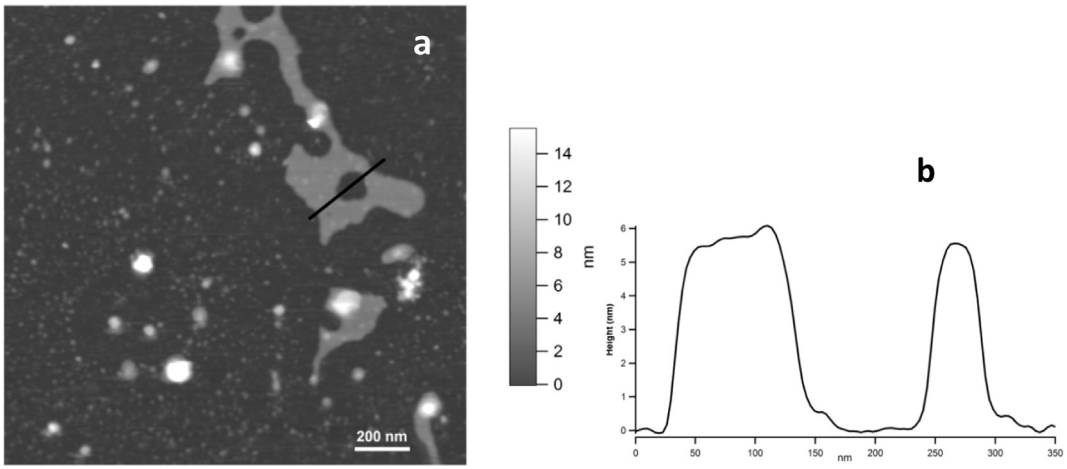

Fig. 5. Self-assembled chitosan-g-ssDNA under ionic strength (150 mM, NaCl) measured by AFM in the liquid state.

charged at lower pH solely, i.e. pH 5 as characterized by zeta potential measurements which give a value of +(65 ± 3) mV.

Overall, these investigations enable to conclude that the formation of micellar structures by chitosan-g-ssDNA is the result of chemical and physical incompatibility between the constitutive segments (Scheme 2). Since these structures are held by hydrophobic interactions and supported by hydrogen bonding, the morphology of the resulting micellar structures is stable to pH and ionic strength variations.

4. Conclusion

We have successfully synthesized chitosan-g-ssDNA hybrids through solid phase supported synthesis. The experimental outcomes reported herein evidence the formation of submicrometer size spherical structures. Resorting to hybridization with the complementary nucleic acid strand to probe intermolecular interactions in parallel to the study of the effect of the pH and ionic strength of the surrounding, the driving force to structure formation is the hydrophobic interaction supported by hydrogen bonding, of high potential for application as drug or gene delivery vectors since the resulting structures are stable to pH and ionic strength variations.

Acknowledgements

The Swiss National Science Foundation (SNSF PPOP2-153025) and the University of Geneva are greatly acknowledged for the financial support.

We are highly thankful for the experimental support of Prof. Michal Borkovec, Dr. Plinio Maroni for their great help with AFM measurements in the liquid state.

The authors are as well thankful to Prof. Helmut Schlaad for analytical ultra centrifugation measurements and Prof. Nicolas Winssinger for access to his equipment, in particular spectrometry.

Appendix A. Supplementary data

Supplementary data related to this article can be found at http://dx.doi.org/10.1016/j.polymer.2015.09.072.

References

[1] A. Domard, Carbohydr. Polym. 84 (2011) 696–703.
[2] a) J. Desbrieres, V. Babak, Soft Matter 6 (11) (2010) 2358–2363;
b) C. Petit, S. Reynaud, J. Desbrieres, Carbohydr. Polym. 116 (0) (2015) 26–33.
[3] a) P. Sorlier, Denuzière, C. Viton, A. Domard, Biomacromolecules 2 (2001) 765–772;
b) B.E. Christensen, I.M.N. Vold, K.M. Vårum, Carbohydr. Polym. 74 (2008) 559–565.
[4] I.K. Voets, A. de Keizer, M.A. Cohen Stuart, Adv. Colloid Interface Sci. 147–148 (2009) 300–318.
[5] G.M. Mekhail, A.O. Kamel, G.A.S. Awad, N.D. Mortada, Int. J. Biol. Macromol. 51 (2012) 351–363.
[6] X.-L. Wang, Y.-L. Zhai, D.-L. Tang, G.-Y. Liu, Y.-Z. Wang, J. Polym. Res. 19 (2012) 9946.
[7] D. Qu, H. Lin, N. Zhang, J. Xue, C. Zhang, Carbohydr. Polym. 92 (2013) 545–554.
[8] N. Elsaid, T.L. Jackson, M. Gunic, S. Somavarapu, Investig. Ophthalmol. Vis. Sci. 53 (2012) 8105–8111.
[9] J. Zhang, M. Li, T. Fan, Q. Xu, Y. Wu, C. Chen, Q. Huang, J. Polym. Res. 20 (2013) 107.
[10] C. Liu, Q. Zhu, W. Wu, X. Xu, X. Wang, S. Gao, K. Liu, Int. J. Nanomed. 7 (2012) 5339–5350.
[11] X. Ding, D.L. Richter, L.M. Matuana, P.A. Heiden, Carbohydr. Polym. 86 (2011) 58–64.
[12] K. Zhang, P. Zhuang, Z. Wang, Y. Li, Z. Jiang, Q. Hu, M. Liu, Q. Zhao, Carbohydr. Polym. 90 (2012) 1515–1521.
[13] X. Niu, L. Wang, P. Chen, X. Li, G. Zhou, Q. Feng, Y. Fan, Macromol. Chem. Phys. 214 (6) (2013) 700–706.
[14] C. Moyuan, J. Haixia, Y. Weijuan, L. Peng, W. Liqun, J. Hongliang, J. Appl. Polym. Sci. 123 (5) (2012) 3137–3144.
[15] F. Teixeira Jr., P. Rigler, C. Vebert-Nardin, Chem. Commun. Camb. (United Kingdom) 11 (2007) 1130–1132.
[16] N. Cottenye, M.-I. Syga, S. Nosov, A. Mueller, L. Ploux, C. Vebert-Nardin, Chem. Commun. 48 (20) (2012) 2615–2617.
[17] D. Kedracki, M. Chekini, P. Maroni, H. Schlaad, C. Nardin, Biomacromolecules 15 (9) (2014) 3375–3382.
[18] a) N. Gour, D. Kedracki, I. Safir, K.X. Ngo, C. Vebert-Nardin, Chem. Commun. Camb. (United Kingdom) 48 (2012) 5440–5442;
b) N. Gour, J. Abraham, M. Chami, A. Castillo, S. Verma, C. Vebert-Nardin, Chem. Commun. Camb. (United Kingdom) 50 (2014) 6863–6865.
[19] H. Lin, W. Wang, C. Xue, M. Ye, Enzyme Microb. Technol. 31 (2002) 588–592.
[20] M.R. Kasaai, Carbohydr. Polym. 79 (4) (2010) 801–810.
[21] a) D.A. Braasch, D.R. Corey, Biochemistry 41 (2002) 4503–4510;
b) G. Grassi, B. Scaggiante, B. Dapas, R. Farra, F. Tonon, G. Lamberti, A. Barba, S. Fiorentino, N. Fiotti, F. Zanconati, M. Abrami, M. Grassi, Curr. Med. Chem. 20 (2013) 3515–3538.
[22] M.H. Ottøy, K.M. Vårum, B.E. Christensen, M.W. Anthonsen, O. Smidsrød, Carbohydr. Polym. 31 (4) (1996) 253–261.
[23] S.T. Balke, A.E. Hamielec, B.P. LeClair, S.L. Pearce, Prod. R&D 8 (1) (1969) 54–57.
[24] C.E. Mora-Huertas, H. Fessi, A. Elaissari, Adv. Colloid Interface Sci. 163 (2) (2011) 90–122.
[25] Weinhold, M., Thesis. 2011: University Bremenn.